Volume 174 • Issues 2–3 • 1 November 2011 • Issn 1385-8947

CHEMICAL ENGINEERING JOURNAL

FEATURED ARTICLES

ENVIRONMENTAL CHEMICAL ENGINEERING
Improved performance of PDMS/ceramic composite pervaporation membranes by ZSM-5 homogeneously dispersed in PDMS via a surface graft/coating approach
Gongping Liu, Fenjuan Xiangli, Wang Wei, Sainan Liu, Wanqin Jin

Chemical Engineering Journal 174 (2011) 668–676

Contents lists available at SciVerse ScienceDirect

Chemical Engineering Journal

journal homepage: www.elsevier.com/locate/cej

Synthesis of monoglyceride through glycerol esterification with lauric acid over propyl sulfonic acid post-synthesis functionalized SBA-15 mesoporous catalyst

Lilis Hermida[a,b], Ahmad Zuhairi Abdullah[a,*], Abdul Rahman Mohamed[a]

[a] School of Chemical Engineering, Universiti Sains Malaysia, 14300 Nibong Tebal, Penang, Malaysia
[b] Department of Chemical Engineering, Universitas Lampung, Bandar Lampung 35145, Lampung, Indonesia

ARTICLE INFO

Article history:
Received 11 May 2011
Received in revised form
12 September 2011
Accepted 14 September 2011

Keywords:
HSO_3SBA-15
Post synthesis grafting
Glycerol monolaurate
Reusable catalyst
Reaction mechanism
Kinetic

ABSTRACT

Monoglyceride synthesis through glycerol esterification with lauric acid over a propyl sulfonic acid functionalized SBA-15 mesoporous catalyst (HSO_3SBA-15) was studied under reduced pressure to continuously remove water formed. Effects of various reaction parameters such as reaction temperature (413–433 K), catalyst loading (1–5%) and glycerol/lauric acid molar ratio (2:1 and 4:1) on lauric acid conversion and products selectivity were successfully elucidated and correlated with reaction scheme and kinetic model. The parent and functionalized SBA-15 were characterized using FT-IR, ammonia chemisorptions, surface analysis, TEM and SEM. Reusability behavior of the catalyst was also demonstrated. Glycerol esterification could be modeled as irreversible parallel reactions and the kinetic data were successfully fitted to a second order kinetic model. The apparent activation energy for monoglyceride formation using a catalyst loading of 5% and glycerol/lauric acid molar ratio of 4:1 was found to be 42 kJ/mol. The HSO_3SBA-15 catalyst could be reused up to four times without significant loss of catalytic activity.

1. Introduction

Monoglyceride has various applications in food products, cosmetics, pharmaceutical formulations, drug delivery systems, oil well drilling operations, etc. [1,2]. Synthesis of monoglyceride through glycerol transesterification with oleic acid methyl ester using solid basic catalysts in solvent free condition was found to be favourable at an elevated temperature (473 K) over rehydrated Al–Mg mixed oxides and Al–Li mixed oxides catalyst that had Bronsted basic sites and Lewis basic sites, respectively [3]. Meanwhile, glycerol transesterification with lauric acid methyl ester over montmorillonite intercalated with lithium hydroxide (LiK10) catalyst and in the presence of tetramethylammonium hydroxide (TMAOH) was recently reported to show excellent performance at a relatively lower temperature (403 K) [4]. However, the use of organic solvent will result in an extra step for its separation during product purification process. Residual solvent content in the product will also limit the application of the monoglyceride, especially when food products are considered [5–7]. Glycerol esterifications with fatty acids at low temperature in solvent free condition using solid acid catalysts such as acidic resins, conventional zeolites, and sulfated iron oxide were reported to be unfavourable for the reaction due to small pore diameters of less than 8 Å [8,9].

To accelerate the reaction involving bulky molecules such as fatty acids, effective solid acids having pore sizes between 20 and 100 Å are required [10,11]. HSO_3SBA-15 catalyst with a pore size of 67 Å synthesized via post synthesis route was found to be an active solid acid catalyst for monoglyceride formation through the glycerol esterification with lauric acid [12]. However, no sufficient information has been reported on the influence of important process variables, reaction pathway and kinetic model on the product formations in the esterification process. As such, a study on these aspects is deemed necessary for the purpose of advancement of knowledge in this research area.

Reaction pathway is essential to be used for constructing a kinetic model that can be applied to predict the changes in amount of specific product obtained during a reaction process. In order to obtain a better understanding of the reaction pathway, several researchers have undertaken various studies on glycerol esterification with different fatty acids and solid acid catalysts to produce monoglycerides [9,13–15]. Based on their observations, it can be concluded that the reaction pathways of glycerol esterification with fatty acid could be modeled either as consecutive reactions (Fig. 1) following the first order kinetic model with respect to glycerol or as irreversible parallel reactions (Fig. 2) following second order kinetic model with respect to fatty acid and glycerol. The reaction orders reported in the open literatures can be summarized in Table 1.

In the present work, glycerol esterification with lauric acid over the HSO_3SBA-15 is reported. The main focus is to investigate the effect of temperature, glycerol/lauric acid molar ratio and catalyst

---

[*] Corresponding author. Tel.: +60 4 599 6411; fax: +60 4 594 1013.
E-mail addresses: chzuhairi@eng.usm.my, azuhairi@yahoo.com (A.Z. Abdullah).

1385-8947/$ – see front matter © 2011 Elsevier B.V. All rights reserved.
doi:10.1016/j.cej.2011.09.072

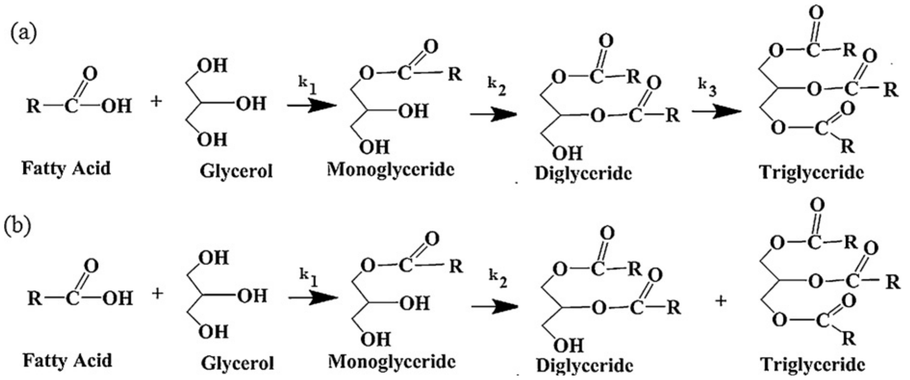

Fig. 1. Consecutive reactions of the glycerol esterification: (a) as proposed by Szelag and Zwierzykowski [13] and, (b) as proposed by Macierzanca and Szelag [14].

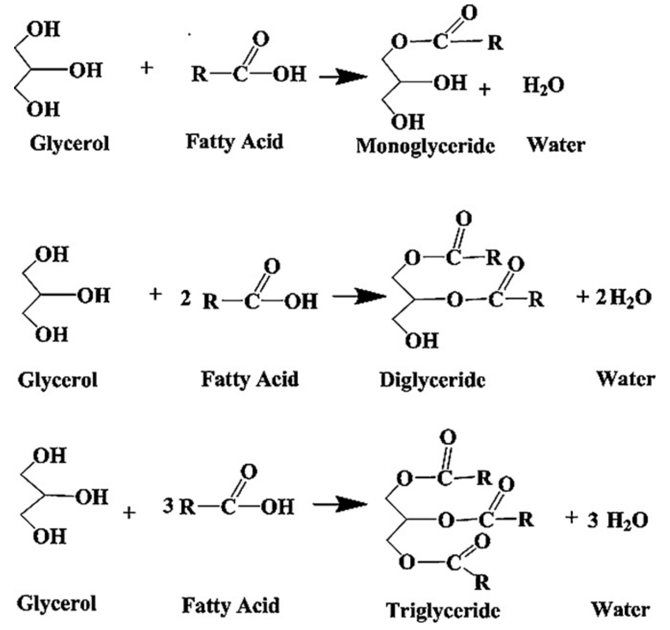

Fig. 2. Irreversible parallel reactions for glycerol esterification with fatty acid as adopted from Sanchez et al. [15].

loading on the products selectivity to gain better understanding of reaction pathway to eventually build a kinetic model for monoglyceride formation. The work also includes model verification, determination of the apparent activation energy of the reaction and reusability study of the catalyst.

2. Experimental

2.1. Catalyst preparation and characterization

SBA-15 mesoporous material was synthesized in the presence of Pluronic P123 which is a triblock co-polymer with a molecular formula of $HO(CH_2CH_2O)_{20}(CH_2CH(CH_3)O)_{70}(CH_2CH_2O)_{20}H$ and a molecular weight of 5800 as the structure-directing agent. After that, the SBA-15 mesoporous material was functinonalized with propylsulfonic acid by refluxing 2 g of SBA-15 materials with 2 mL of 3-mercaptopropyl trimethoxysilane (MPTMS). Then, soxhlet extraction was carried out for 20 h, followed by mild oxidation using H_2O_2 to form HSO_3SBA-15. The preparation methods of SBA-15 material and HSO_3SBA-15 catalyst were thoroughly described in a previously published article [15]. The parent SBA-15 mesoporous material and HSO_3SBA-15 catalyst were then characterized using FT-IR spectroscopy, pulse chemisorption followed by temperature programmed desorption (TPD) of NH_3, surface area analysis, TEM analysis and SEM analysis. Meanwhile, Fourier transform infrared (FT-IR) spectrum was used to detect the presence of organosulfonic acid group which was grafted on SBA-15 mesoporous material. The FT-IR spectroscopy was performed using a Perkin Elmer 2000 Fourier transformed infrared (FT-IR) system.

Acidity characterization of the catalysts involved pulse chemisorption of ammonia followed by its temperature-programmed desorption (TPD) using micromeritics Autochem II 2920 instrument. The sample was first activated by heating to 150 °C in helium for 2 h, and then cooled down to 127 °C. During the ammonia chemisorption step, 5 injections of ammonia were dosed onto the sample (to ensure the sample was saturated). After saturation, the temperature was subsequently increased from 127 to 427 °C to perform the TPD of NH_3 analysis.

Pore size distribution was obtained from N_2 adsorption–desorption isotherms of the prepared SBA-15 and HSO_3SBA-15 samples. The N_2 adsorption–desorption measurements were performed using a Quantachrome Autosorb-1 equipment. Prior to the experiment, the samples were degassed ($P < 10^{-1}$ Pa) at 270 °C for 6 h. Surface area was calculated using the BET method (S_{BET}) and pore size distribution was determined using the Barrett–Joyner–Halenda (BJH) model applied to the desorption branch of the isotherm. The micropore area (S_{μ}) was estimated using the correlation of *t*-Harkins and Jura (*t*-plot method).

The TEM images were obtained using Philips CM 12 transmission electron microscope. The sample of about 0.08 g was first dispersed in 5 ml ethanol. Then, the solution was vigorously shaken for a while. Subsequently, a small amount of the solution was taken

Table 1
Summary of published kinetic models for glycerol esterification with fatty acids reaction over various solid acid catalysts.

Type of catalysts	Fatty acids (FA)	G/FA[a] molar ratio	Reaction pathways	Rate reaction expression[b]	Refs.
Na or K soaps	Lauric acidMyristic acidPalmitic acidStearic acid	1:1	Consecutive reactions	$-r_G = k_1C_G\, r_{Mono} = k_1C_G - k_2C_{Mono}$	[13]
Zinc carboxylates	Lauric acidMyristic acidPalmitic acidStearic acid	1:1	Consecutive reactions	$-r_G = k_1C_G\, r_{Mono} = k_1C_G - k_2C_{Mono}$	[14]
Sulfated iron oxide	Oleic acid	1:1	Parallel reactions	$-r_{FA} = -(1/W)(dC_{FA}/dt) = k_1C_GC_{FA}$	[9]
Zeolite (faujasite)	Oleic acid	1:3, 1:1 and 3:1	Parallel reactions	$-r_{FA} = -(1/W)(dC_{FA}/dt) = k_1C_GC_{FA}$	[15]

[a] G/FA = glycerol/fatty acid molar ratio.
[b] $-r$ = rate of reaction, C_x = concentration of reactant x, k_1 = rate constant for forward reaction, k_2 = rate constant for reverse reaction, W = weight of catalyst.

Table 2
Experimental conditions used for the kinetic study.

Variable	Value
Catalyst concentration with respect to reactants (wt.%)	1, 3, 5
Glycerol/fatty acid molar ratio	2:1, 4:1
Operating pressure (cm Hg)	50.8

by using a micro pipette and dropped on a metal grid for the analysis. Meanwhile, scanning electron microscopy (SEM) imaging was performed using a Leo Supra scanning electron microscope (model 35 VP-24-58) at 3.00 kV. The SEM images were taken directly from these samples without altering or coating.

2.2. Esterification of glycerol with lauric acid

The glycerol esterification processes were usually carried out under continuous water removal. Water removal during esterification is needed as it is formed as a side product and will inhibit the activity of a solid acid catalyst. It can also promote reverse reaction. Besides, esterification is an equilibrium limited reaction in which full conversion can only be achieved when one of the products is removed [16]. In this study, esterification of glycerol with lauric acid using different HSO_3SBA-15 catalyst loadings, lauric acid/glycerols molar ratios and reaction temperatures was carried out in a batch system with continuous removal of water by working at a low pressure of 50.8 cm Hg and without the use of any solvent.

Typically, the esterification was carried out in a two-necked flask reactor equipped with a stirrer, a thermometer, a tube connected with a vacuum pump and a tube for sampling. The reactants i.e. lauric acid, glycerol as well as the catalyst were first added to the reactor. Before any experiment was started, the system was flushed with nitrogen to create inert environment. The reaction mixture was then heated to a certain temperature under a reduced pressure of 50.8 cm Hg. Stirring at 750 rpm was then started and the reactants were stirred for up to 7 h. Summary of the experimental conditions is given in Table 2.

2.3. Reusability study

In the reusability study of the HSO_3SBA-15 catalyst, 5 wt.% of fresh catalyst with respect to the initial reactants was used for the reaction performed at 433 K for 6 h and the glycerol/lauric acid molar ratio was set at 4:1. After the experiment, the catalyst was filtered from the catalytic reaction mixture, successively washed with toluene and acetone and then dried in an oven at 373 K. Then, the catalyst was reused for the subsequent esterification runs using the same reaction conditions. Such reusability experiments were repeated for 4 times and the activity was measured based on conversion of lauric acid and selectivity to monoglyceride.

2.4. Product analysis

Mono-, di- and triglycerides were analyzed based on gas chromatography method using Agilent 7820A and with a capillary column (15 m × 0.32 mm × 0.10 μm CP Sil 5CB). The analysis method was adopted from a published work [17]. The detector and injector temperatures were 380 °C and 250 °C, respectively. The column temperature was set at 80 °C for 1 min and was then programmed at 15 °C/min to 330 °C, which was then maintained constant for 2 min. 100 μL of sample was then transferred from the reactor into a sample vial containing 100 μL of water and 100 μL of methyl acetate. Next, the mixture was vortexed and the organic phase was separated by means of centrifugation. 20 μL organic phase was then dissolved in 480 μL acetone and 100 μL of 0.2 M pentadecanoic acid as the internal standard. The sample was then directly injected into the gas chromatograph. Conversion was calculated based on the amount of lauric acid converted in the reaction leading to the formation of mono-, di-, and triglycerides. Meanwhile, the selectivity of monoglyceride, diglyceride and triglyceride were expressed based on the ratio of the ester to all the reaction products (corrected by the reaction coefficients), as given in Eqs. (1), (2) and (3) [7];

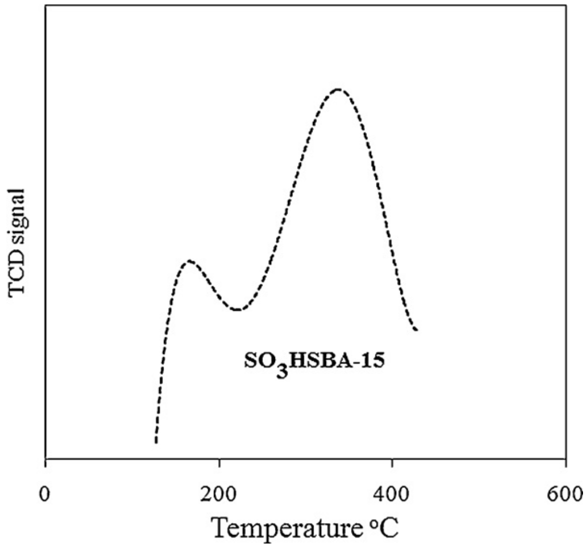

Fig. 3. NH_3 temperature-programmed desorption profile of HSO_3SBA-15 catalyst.

$$S_M(\%) = \frac{C_{Monoglyceride}}{C_{Monoglyceride} + 2C_{Diglyceride} + 3C_{Triglyceride}} \times 100 \quad (1)$$

$$S_D(\%) = \frac{2C_{Diglyceride}}{C_{Monoglyceride} + 2C_{Diglyceride} + 3C_{Triglyceride}} \times 100 \quad (2)$$

$$S_T(\%) = \frac{3C_{Triglyceride}}{C_{Monoglyceride} + 2C_{Diglyceride} + 3C_{Triglyceride}} \times 100 \quad (3)$$

3. Results and discussion

3.1. Characterization of the SBA-15 and HSO_3SBA-15 catalysts

The evidence that the functionalized SBA-15 material indeed contained propyl sulfonic group was provided by FT-IR spectrum analysis as explained in detail in our article [12]. Sulfonic acid silicas are a class of solid Bronsted acid catalyst that contains tethered organo-sulfonic acid groups [18,19]. Acidity analysis of the parent SBA-15 and the catalyst using pulse chemisorptions and TPD of NH_3 in the region of 127–427 °C confirmed that the HSO_3SBA-15 catalyst contained weak and medium Bronsted acid sites with an overall concentration of 42 μmol/g. NH_3-TPD profile of the catalyst is presented in Fig. 3. The locations of the two the peaks are in agreement with results reported by other researchers [19]. They performed acid sites analysis in the temperature range from 50 to 527 °C and found out that the HSO_3SBA-15 catalyst showed two peaks of acid sites i.e. weak and medium acid sites in the NH_3-TPD curves related to the desorption of NH_3 on the region of 127–427 °C. At higher temperature (427–527 °C), the propyl sulfonic groups began to decompose. Meanwhile, the amount of acid sites in the SBA-15 without acid functionalization was not detected, to the confirmation that SBA-15 is indeed a neutral material.

The surface area analysis results of SBA-15 and HSO_3SBA-15 are shown in Table 3. SBA-15 was found to be a mesoporous material with a surface area of 542 m^2/g and an average pore size diameter of 59 Å. After the post-synthesis functionalization, it was found that HSO_3SBA-15 catalyst had a surface area of 607 m^2/g

Table 3
Surface analysis results of SBA-15 and HSO_3SBA-15 catalyst.

Surface analysis	SBA-15	HSO_3SBA-15
Total surface area[a] (m^2/g)	542	607
Total pore volume (cm^3/g)	0.795	1.018
Micro pore area[b] (m^2/g)	149	79
Meso pore area (m^2/g)	393	528
Average pore size (Å)	59	67

[a] Using the BET equation (S_{BET}),
[b] Using the correlation of *t*-Harkins and Jura (*t*-plot method)

and an average pore diameter of 67 Å that were larger compared to those of the parent SBA-15 material. The increase in the pore size after the functionalization indicated that the preparation conditions used allowed the enlargement of mesoporous structure of the SBA-15 and grafting of sulfonic acid groups on the mesoporous surface at the same time [20]. Besides, the mesopore area of the catalyst (528 m^2/g) was higher than that of the parent SBA-15 material (393 m^2/g). Meanwhile, the catalyst had a micro pore area of 79 m^2/g that was lower than that of the parent material i.e. 149 m^2/g. This finding suggested that the catalyst preparation conditions allowed the restructuring of the hexagonal structures in the HSO_3SBA-15 catalyst. This restructuring resulted in significant disappearance of micropore structures.

Furthermore, evidences that SBA-15 and HSO_3SBA-15 catalyst mainly had mesoporous structures were confirmed by results of N_2 adsorption-desorption measurement and analysis of pore size distributions of the SBA-15 and H SO_3SBA-15 catalysts with the desorption branch using BJH method. As shown in Fig. 4. Fig. 4(a), nitrogen adsorption–desorption isotherm curves for the parent SBA-15 and modified SBA-15 exhibited type IV isotherms, implying that they were materials with sufficiently ordered mesostructures [21]. Meanwhile, Fig. 4(b) shows their pore size distributions in which pore size at the maximum peak in SBA-15 and HSO_3SBA-15 in the range of mesopore structures. In addition, Fig. 4(b) confirms that the HSO_3SBA-15 catalyst had more defined pore structure with larger pore size at the maximum peak than that of the parent SBA-15.

TEM and SEM images of SBA-15 and HSO_3SBA-15 catalyst are presented in Fig. 5. TEM images of the parent SBA-15 and the catalyst showed that in general their structures were well-ordered mesoporous material as shown in Fig. 5(a) and (b), respectively. The SEM images of parent SBA-15 and the catalyst presented in Fig. 5(c) and (d), respectively, reveal that their structures had fibrous and porous-type morphology.

3.2. Effects of reaction parameters on the catalyst performance

This section discusses the effect of reaction temperature, catalyst loading and glycerol/lauric acid molar ratio on reaction products. Next, detailed examination on the reaction pathways of glycerol esterification with lauric acid over catalyst is attempted. This leads to the identification of the sequence of the reaction steps. In this work, experimental errors in the measurement of concentration were within ±4%. However, particular focus was only given to general trends in the results rather than specific data points. As such, trend lines were deemed sufficient to show the process behaviors.

3.2.1. Effect of reaction temperature

Considering HSO_3SBA-15 catalyst had an average pore diameter of about 67 Å [12], diffusion limitation had been excluded for the esterification of glycerol with fatty acid [11]. Several catalytic tests were carried out at various reaction temperatures (413 K, 423 K, and 433 K) using a constant glycerol/lauric acid molar ratio of 4:1 and a constant catalyst loading of 5%. The effects of reaction temperature on lauric acid conversion and reaction products i.e. monoglyceride, diglyceride and triglyceride yields are shown in Fig. 6. Lauric acid conversion significantly increased with the increase in the reaction temperature in which the conversion increased. For example, it increased from 75% at 413 K to 85% at 423 K then to 95% at 433 K at a reaction time of 7 h. These figure suggested the high potential of the mesoporous catalyst in catalyzing the reaction. This observation also suggested that by increasing the temperature, kinetic energy of glycerol and lauric acid was higher so that the number chemisorptions on the active sites and subsequently effective interaction between the reactant molecules were enhanced [22]. By the presence of acid sites either in the inner or the outer pores of HSO_3SBA-15 catalyst, the higher effective collisions led to the significant increase in lauric acid conversion. The continuous removal of water from the reacting system also helped in improving the conversion as the reverse reaction was suppressed.

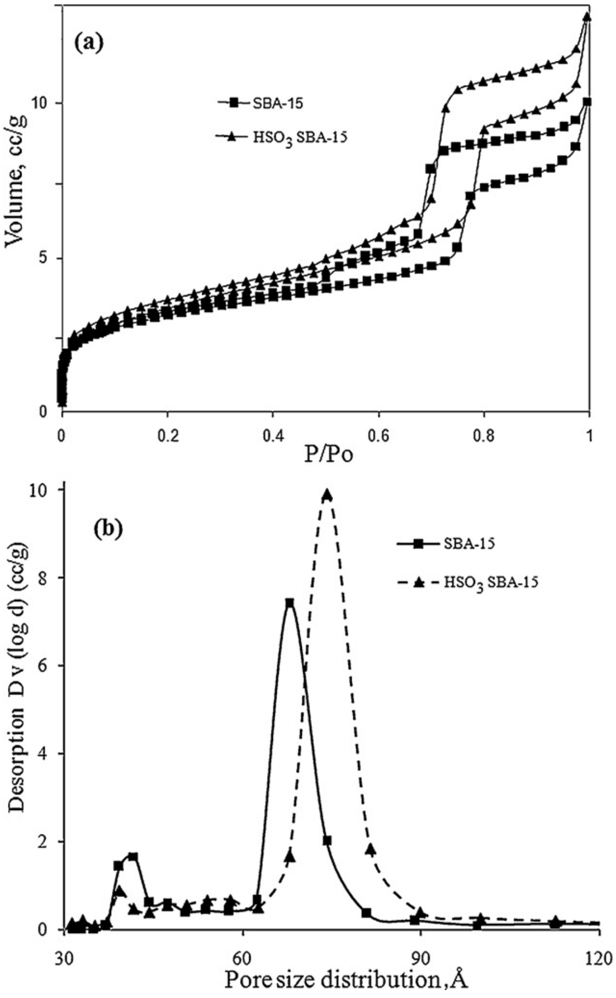

Fig. 4. N_2 adsorption–desorption isotherm curves: (a) and pore size distribution curves: (b) of SBA-15 and HSO_3SBA-15 catalyst.

The increase in reaction temperature also significantly improved monoglyceride yield, i.e. from 50% at 413 K, to 64% at 423 K, then to 68% at 433 K in the same period of time. However, effect of reaction temperature on other products such as diglyceride and triglyceride was quite minor. This result indicated that the glycerol esterification reaction mainly occurred in the internal mesopores of the catalyst, which favoured the monoglyceride formation. Meanwhile, the formations of diglyceride and triglyceride which are bulkier than monoglyceride were restricted [10,11]. It could also be contributed by steric effects post by the

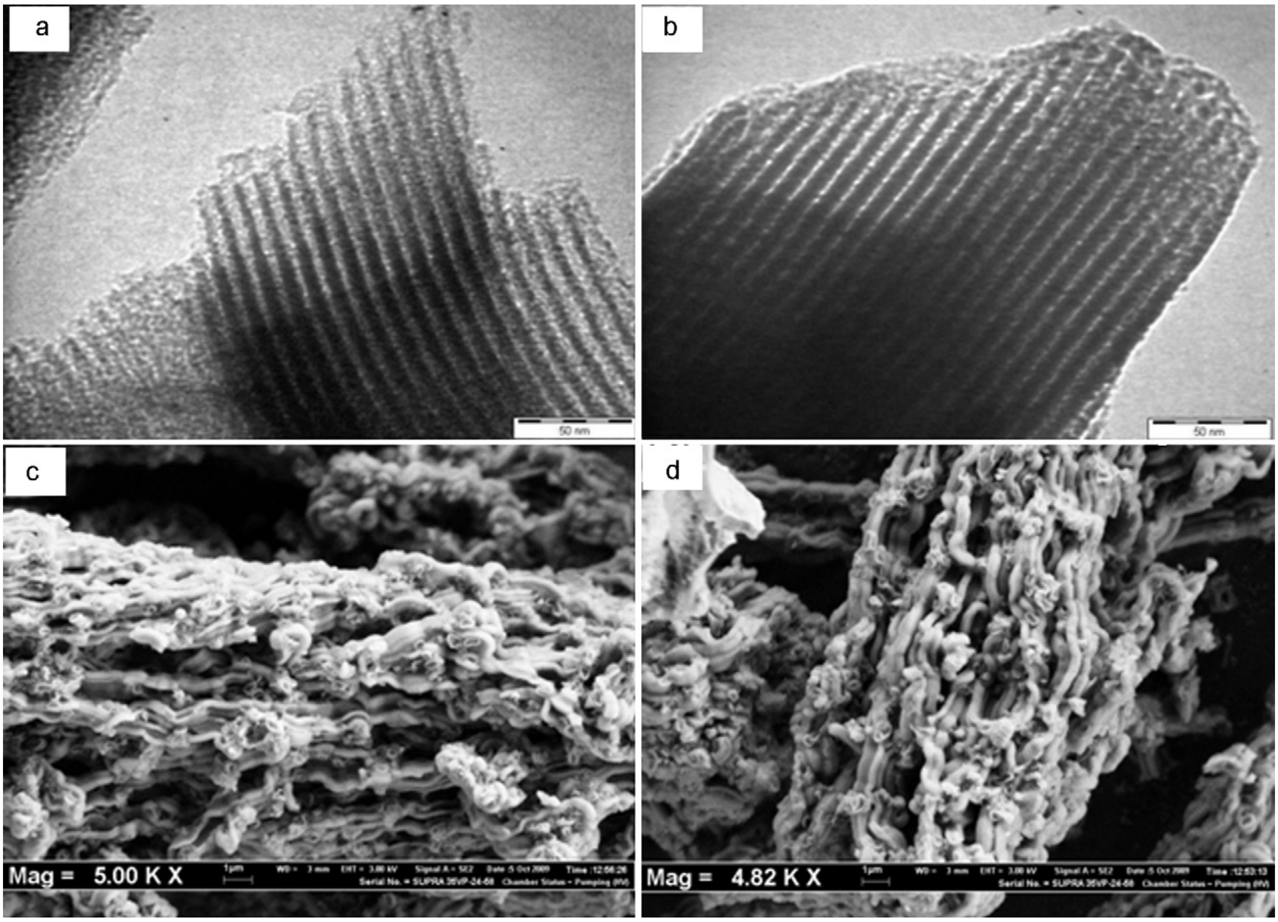

Fig. 5. TEM images of (a) SBA-15, (b) HSO_3SBA-15, and SEM images of (c) SBA-15 and (d) HSO_3SBA-15.

earlier attached fatty acid end of the monoglyceride and diglyceride molecules.

3.2.2. *Effect of catalyst loading*

Several catalytic tests were also conducted at 433 K with different HSO_3SBA-15 catalyst loadings (1 wt.%, 3 wt.% and 5 wt.% with respect to the reactants) using a constant temperature of 433 K and a constant glycerol/lauric acid molar ratio of 4:1. Effects of catalyst loading (W) on lauric acid conversion and products of the reactions can be seen in Fig. 7. Results in Fig. 7(a) indicate that when the catalyst loading was increased from 1 wt.% to 3 wt.% at reaction time of 7 h, lauric acid conversion increased from 90% to 95%. This observation suggested that the increase in catalyst loading from 1 wt.% to 3 wt.% increased the number of acid sites available for the reaction as the catalyst had an acid site concentration of 42 μmol/g as confirmed in the characterization results. However, with an increase in the catalyst loading from 3% to 5 wt.%, no further enhancement in the conversion was observed, especially at longer reaction time. This could be attributed to the fact that beyond a certain catalyst loading, there was an excess of catalyst acid sites than actually required by the reactant molecules so that the conversion levelled off [23]. Similar trend was also demonstrated by glycerol transesterification reaction [4] to suggest that the beneficial role of higher catalyst loading was only limited to low reactant conversion.

Fig. 7(b) shows that at a reaction time of 7 h, monoglyceride yields remained virtually stable when the catalyst loading was increased from 1 wt.% to 3 wt.%. These results indicated that the occurrence of reaction in the internal mesopores of HSO_3SBA-15 catalyst did not increase by increasing the catalyst loading from 1 wt.% to 3 wt.%. However, diglyceride yield slightly increased with the increase in the catalyst loading from 1 wt.% to 3 wt.%. This result was attributed to the occurrence of reaction in the external pores of the catalyst so that diglyceride formation was improved. However, if the catalyst loading was increased from 3% to 5 wt.%, monoglyceride yield was found to improve from 60% to 68% while diglyceride yield decreased from 30% to 27% and triglyceride yield was rather stable at low level. This observation indicated that by increasing the catalyst loading from 3% to 5 wt.%, the occurrence of reaction in the internal mesopore of HSO_3SBA-15 catalyst was more frequent rather than in the external pore of the catalyst. As such, the formation of monoglyceride was more favourable rather than that of diglyceride or triglyceride.

3.2.3. *Effect of initial glycerol/lauric acid molar ratio*

In order to investigate the effect of glycerol/lauric acid molar ratio on the esterification reaction, catalytic tests were also performed on the same catalyst but with different glycerol/lauric acid molar ratios, i.e. 2:1 and 4:1 at 433 K using a constant catalyst load of 5 wt.%. Fig. 8 shows the effect of glycerol/lauric acid molar ratio on the lauric acid conversion and the reaction products. As can be seen in the figure, the effect of glycerol/lauric acid molar ratio on the lauric acid conversion was insignificant when the glycerol/lauric acid molar ratio was increased from 2:1 to 4:1, especially after 3–7 h of reaction. However, for the reaction product, monoglyceride yield significantly increased from 58% to 68%, while diglyceride yield experienced a decrease from 35% to 23%. However, triglyceride yield remained stable at very low level (below 2%).

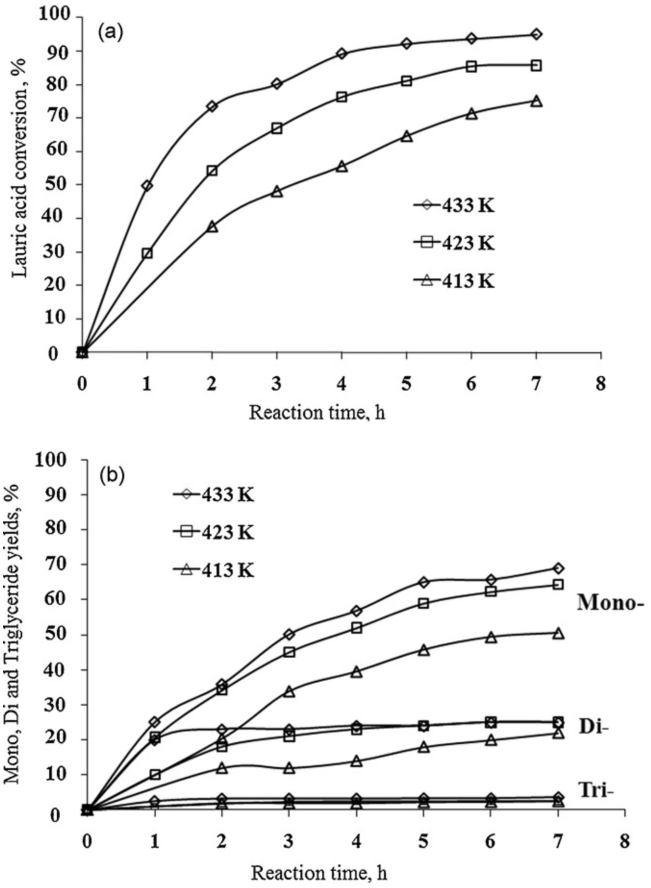

Fig. 6. Effect of reaction temperature on glycerol esterification using a glycerol/lauric acid molar ratio of 4:1 and a catalyst loading of 5 wt.%.

The increase in monoglyceride yield at higher molar ratio of glycerol to lauric acid was attributed to a higher chance for lauric acid to react with glycerol mainly in the pores of HSO_3SBA-15 mesoporous catalyst to produce and allow the diffusion of monoglyceride. This observation result was in agreement with the glycerol esterification with lauric acid over SO_3HMCM-41 mesoporous catalyst [24]. Meanwhile, Machado et al. [5,6] reported that the increase in glycerol/lauric acid molar ratio resulted in a decrease in monoglyceride yield in glycerol esterification reaction with lauric acid catalyzed by zeolite. This was because the small pore size of zeolite (below 20 Å) retarded the formation and diffusion of bulky molecules such as monoglyceride [10]. As such, the reaction mainly occurred on the external pore of the catalyst that provided larger opportunity for the formation of the bulkier molecules (diglyceride and subsequently trigyceride).

3.3. *Reusability of HSO_3SBA-15 catalysts*

Catalyst reusability is a crucial aspect in practical monoglyceride production. In the present study, the HSO_3SBA-15 catalyst was tested with respect to the reusability in the glycerol esterification with lauric acid at 433 K for 6 h using the catalyst amount of 5% (with respect to weight of initial reactant). After the catalytic esterification reaction, the used catalyst was recovered by filtering from the reaction mixture, washed with solvent and dried at 100 °C. The catalyst was then reused for another glycerol esterification under the same operating conditions.

As seen in Fig. 9, the HSO_3SBA-15 catalyst showed a rather good activity retention in several cycles of usage. The catalyst retained up to 90% from its initial conversion of 93.7% and up to 68.7%

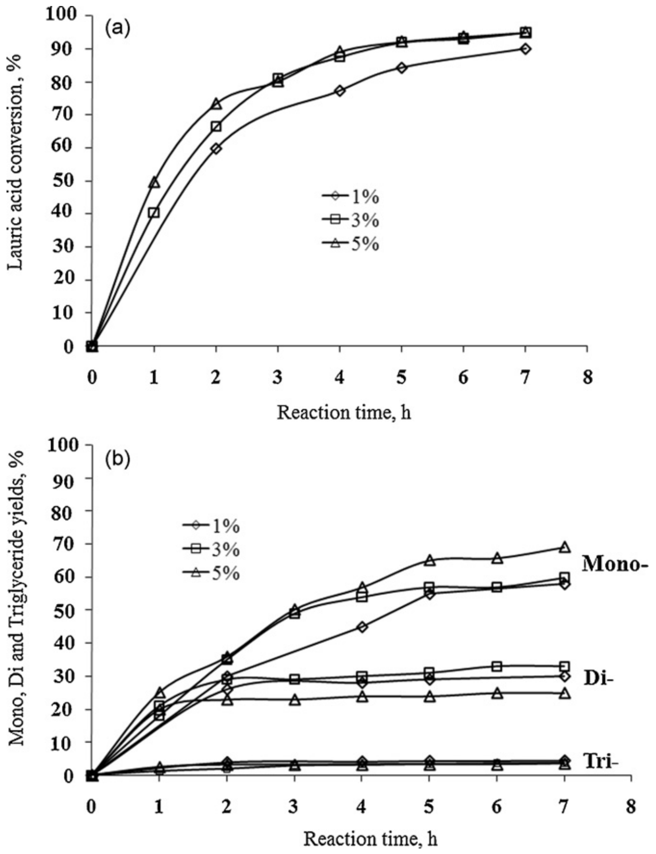

Fig. 7. Effect of catalyst loading on glycerol esterification using a glycerol/lauric acid molar ratio of 4:1 at 433 K.

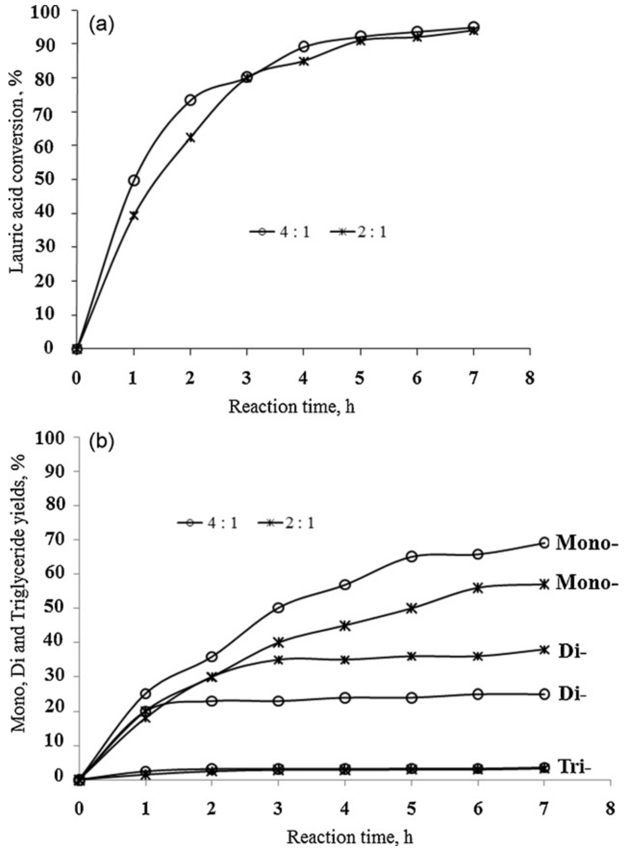

Fig. 8. Effect of glycerol/lauric acid molar ratio on glycerol esterification at 433 K using a HSO_3SBA-15 catalyst loading of 5 wt.%.

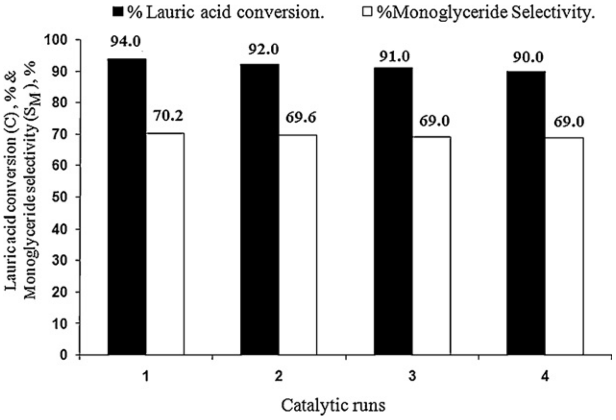

Fig. 9. Lauric acid conversion and monoglyceride selectivity shown by HSO_3SBA-15 catalyst when used in four successive runs.

from its initial monoglyceride selectivity of 70.2% in the fourth cycle without experiencing significant deactivation. The result was attributed to post synthesis-grafting method applied in this catalyst preparation method leading to covalent attachment of organo sulfonic acid groups to porous silica frameworks without the risk of pore blockage or leaching of the grafted component [25–29]. A minor decrease in lauric acid conversion and monoglyceride selectivity could be attributed to minor deactivation to some active sites (sulfonic acid group) or defects in the mesoporus structure of the catalyst. In this respect, the significant role of small loss in the catalyst amounts used from run 1 to run 4 could be ruled out as catalyst amounts between 3 and 5 wt.% did not pose significant different in the activity as proven by results in Fig. 7. The activity retention of HSO_3SBA-15 in present study was comparable to that reported in the literature [30] utilising similar catalyst for the synthesis of chromenes from chromanol.

3.4. *Reaction pathway*

To get a better understanding of the reaction pathways of glycerol esterification with lauric acid, formations of reaction products i.e. monoglyceride, diglyceride and triglyceride, as a function of time at different temperatures, catalyst loadings and initial glycerol/lauric acid molar ratios were scrutinized. Monoglyceride, diglyceride and triglyceride yields as functions of reaction time at different temperatures are shown in Fig. 6. The profiles suggest that the reaction between lauric acid and glycerol mainly formed monoglyceride. Maximum monoglyceride yield with the decrease in the monoglyceride yield after reaching a certain maximum point are not observed in the figure. These results indicated that diglyceride was directly produced from the esterification reaction between lauric acid and glycerol and not from the transesterification reaction between monoglyceride and glycerol. The latter reaction is known to be a base-catalyzed reaction [4].

The same explanation was applicable in the case of triglyceride formation in which triglyceride was also directly synthesized from the reaction between lauric acid and glycerol and not from the reaction between diglyceride and glycerol as there was no significant decrease in diglyceride yield as noted in the figure. Thus, the reaction pathways of the esterification of glycerol with lauric acid in this study were deemed to follow irreversible parallel reactions in which reaction mechanism involved a series of glycerol esterification with lauric acid reactions that occurred at the same time to form monoglyceride, diglyceride and triglyceride. It can be concluded from Fig. 6 that the increase in reaction time at different temperatures caused positive effects on monoglyceride, diglyceride and triglyceride formations.

Table 4
Specific rate constants for the second-order kinetic model.

Temperature (K)	Specific rate constant, k_s (L/(mol g_{cat} h))
413	0.0046
423	0.0069
433	0.0079

These conclusions were consistent with the products yield plots as shown in Figs. 7 and 8 for different catalyst loadings and for different glycerol/lauric acid molar ratios, respectively. Initially, monoglyceride significantly increased with reaction time until 5 h of reaction. Then the monoglyceride formation would remain stable until a reaction time of 7 h as shown in the figures. While diglyceride and triglyceride yields increased only for the first 2 h, subsequently the yields were found to be stable for reaction times between 2 and 7 h. These observations indicated that lauric acid and glycerol were mainly consumed to form monoglyceride, suggesting that the esterification took place mostly in the internal mesopores rather than in the external pores of the catalyst.

3.5. *Kinetic model of monoglyceride formation*

As the reaction pathways followed irreversible parallel reactions, the reaction rate was calculated based on second order kinetic model with respect to glycerol and fatty acid. The amounts of lauric acid consumed in the reaction to form monoglyceride at any time were considered to be equal to the amounts of glycerol consumed as given in Eq. (4);

$$C_{G0}X_{G0} = C_{FA0}X_{FA0} \tag{4}$$

$$M = \frac{C_{G0}}{C_{FA0}} \tag{5}$$

If X_M = monoglyceride yield, then;

$$C_G = C_{FA0} - C_{FA0}X_M \tag{6}$$

and,

$$C_{FA} = C_{G0} - C_{FA0}X_M \tag{7}$$

where

$-r_{FA}$ = rate of reaction, mol/(g_{cat} h L)
W = catalyst weight, g
C_G = glycerol concentration, mol/L
C_{FA} = fatty acid concentration, mol/L
C_{G0} = initial glycerol concentration, mol/L
X_{G0} = initial glycerol conversion to monoglyceride
C_{FA0} = initial fatty acid concentration, mol/L
X_{FA0} = initial fatty acid conversion to monoglyceride
M = molar ratio of glycerol to fatty acid
k = overall rate constant, L/(mol h)
k_s = specific rate constant, L/(mol h)
t = time, h

By substituting Eqs. (4)–(7) in the second order kinetic model from Table 1, $-r_{FA} = -(1/W)(dC_{FA}/dt) = k_1 C_G C_{FA}$, an expression in Eq. (8) is obtained;

$$\ln\left\{\frac{(M - X_M)}{[M(1 - X_M)]}\right\} = C_{FA0}W(M - 1)kt \tag{8}$$

The specific rate constants (k_s) at various temperatures were calculated based on Eq. (8) by applying nonlinear regression methods and the results are summarized in Table 4. The data correctly suggest the increasing trend of the reaction rate constant with reaction temperature. This result indicated that the reaction was more favourable with the increase in temperature as reactant molecules had higher kinetic energy at the higher temperature. As a result, collisions between reactant molecules in the inner pores of the catalyst were more frequent. This situation would speed up the rate of monoglyceride formation [22]. However, too high temperature (beyond 200 °C) could result in the side reactions leading to degradation of fatty acids as well as the monoglyceride [4].

The activation energy and pre-exponential factor for monoglyceride formation were obtained using an Arrhenius type function by plotting ($\ln k_s$) vs ($1/T$). In this study, the experiment was repeated several times so that odd data could be identified and discarded. Finally, the $\ln(k)$ vs ($1/T$) plot resulted in a linear line with an R^2 value of 0.93 which was regarded as sufficiently high to indicate the accuracy of the model used. The value of activation energy (E) and pre-exponential factor (A) were found to be 10 kcal/mol (42 kJ/mol) and 655 L/(mol g_{cat} h), respectively. The activation energy obtained over the HSO_3SBA-15 catalyst for monoglyceride formation in the glycerol esterification with lauric acid was lower than that obtained over zinc carboxylates catalyst, i.e. 51 kJ/mol, as reported in the literature [14]. This result indicated that the glycerol esterification catalyzed by HSO_3SBA-15 catalyst required a significantly lower energy for monoglyceride formation than that catalyzed by zinc carboxylates. The reaction in this study was also more influenced by an increase in the reaction temperature [4]. The lower activation energy could be attributed to the high surface area and mesoporous structures of HSO_3SBA-15 catalyst which was accessible to bulky molecules of lauric acid to more selectively react with glycerol to produce monoglyceride. Besides, the macropores on the external surface of the catalyst could assist the reaction. It should be borne in mind that the sulfonic acid functionalization was possible on the internal and external surface as this acid group will attach to surface silanols [24].

Furthermore, the activation energy obtained in glycerol esterification with oleic acid for monoglyceride formation was 26.5 kJ/mol over ultrastable NaY-zeolite catalyst containing micro and meso structures [15]. However, the selectivity to monoglyceride was rather poor. This result could be attributed to the small pore size that would pose some geometric constraint to the reactant as well as the product [6]. Meanwhile, superacidity catalysts having much small particle characteristics with sizes below 100 nm, such as sulfated iron oxide, lead oxide, zinc chloride, cobalt chloride and tin chloride gave higher activation energies of 68.2 kJ/mol, 66.8 kJ/mol, 78.8 kJ/mol, 74.0 kJ/mol, and 78.3 kJ/mol, respectively. The same value was reported to be at 89.3 kJ/mol for the reaction without catalyst (fatty acid can act as autocatalyst) [9]. It could therefore be concluded that the presence of solid acid catalysts reduced energy barrier for the monoglyceride production from oleic acid and further reduction could be achieved using a catalyst having mesopore structures as monoglyceride would be favourably formed in the internal pores of the catalyst. This was supported by the characterization results in this study that showed predominately mesopores rather than micropores that contributed to the overall surface area.

With the kinetic parameters obtained, the kinetic model of rate expression for monoglyceride formation in glycerol esterification with lauric acid over HSO_3SBA-15 catalyst was proposed as given in Eq. (9).

$$-r_{FA} = 654.64\ \exp\left(\frac{-9702}{RT}\right) C_G C_{FA} \quad \text{mol}/(\text{L g}_{cat}\ \text{h}) \tag{9}$$

Monoglyceride yields under various conditions as predicted using the kinetic model proposed were found to satisfactorily fit the experimental ones obtained in this study. It clearly shows a good agreement between the model predictions and experimental results under various conditions, with $R^2 = 0.96$. The result evidently showed the sufficient validity of the proposed second order kinetic model to represent the reaction. This result indirectly validated the assumption that the reaction followed an irreversible parallel reaction mechanism with second order of reaction.

4. Conclusions

Behaviors of glycerol esterification with lauric acid over HSO_3SBA-15 in the temperature range between 413 and 433 K, catalyst loading from 0 to 5% w/w with respect to the reactants, and glycerol/lauric acid molar ratio of 2:1 and 4:1 were successfully investigated in a stirred batch reactor under low pressure. Monoglyceride yield was found to increase with an increase in the temperature, catalyst loading and molar feed ratio. HSO_3SBA-15 catalyst could be repeatedly used for up to four cycles without experiencing significant deactivation. The glycerol esterification reaction pathways were considered to be irreversible parallel reactions for the formation of monoglyceride, diglyceride and triglyceride under these conditions. Thus, second order kinetic model with respect to glycerol and lauric acid gave a better representation of kinetic behavior. The estimated rate constant increased with the increase in temperature to correctly indicate that the reaction was more favourable with the increase in temperature. By using Arrhenius type function, the activation energy for monoglyceride formation through the esterification was found to be 42 kJ/mol (or 10 kcal/mol). Meanwhile, kinetic model of rate of expression was $-r_{FA} = 654.64 \exp(-9702/RT) C_G C_{FA}$ mol/(L g_{cat} h) which could be satisfactorily used to predict the progressive changes in amount of monoglyceride formed during the reaction.

Acknowledgments

The contribution of Prof. Subhash Bhatia in shaping up catalysis research capability at School of Chemical Engineering, Universiti Sains Malaysia needs special acknowledgement. A Short Term and a Research University (RU) grant from Universiti Sains Malaysia to support this work are also gratefully acknowledged.

References

[1] L. Hermida, Acid functionalization of SBA-15 mesoporous catalyst for glycerol esterification to monoglyceride, MSc thesis, Universiti Sains Malaysia, Malaysia, 2010.
[2] R. Nakamura, K. Komura, Y. Sugi, Catal. Commun. 9 (2008) 511–515.
[3] A. Corma, S.B.A. Hamid, S. Iborra, Velty, J. Catal. 234 (2005) 340–347.
[4] A.Z. Abdullah, T.Y. Wibowo, R. Zakaria, Chem. Eng. J. 167 (2011) 328–334.
[5] M.S. Machado, J. Pérez-Pariente, E. Sastre, D. Cardoso, A.M. de Guereñu, Appl. Catal. A 203 (2000) 321–328.
[6] M.S. Machado, D. Cardoso, J. Perez-Pariente, E. Sastre, A.M. de Guereñu, Stud. Surf. Sci. Catal. 130 (2000) 3417–3422.
[7] Y. Pouilloux, S. Abro, C. Van hove, J. Barrault, J. Mol. Catal. A 149 (1999) 243–254.
[8] E. Heykants, W.H. Verrelst, R.F. Parton, P.A. Jacobs, Stud. Surf. Sci. Catal. 105 (1997) 1277–1284.
[9] F.S. Gurner, J. Am. Chem. Soc. 73 (1996) 347–351.
[10] J. Perez-Pariente, I. Diaz, F. Mohino, E. Satre, Appl. Catal. A 254 (2003) 173–188.
[11] K. Wilson, J.H. Clark, Pure Appl. Chem. 72 (2000) 1313–1319.
[12] L. Hermida, A.Z. Abdullah, A.R. Mohamed, J. App. Sci. 10 (24) (2010) 3199–3206.
[13] H. Szelag, W. Zwierzykowski, Lipid 100 (1998) 302–307.
[14] A. Macierzanka, H. Szelag, Ind. Eng. Chem. Res. 43 (2004) 7744–7753.
[15] N. Sanchez, M. Martınez, J. Aracil, Ind. Eng. Chem. Res. 36 (1997) 1524–1528.
[16] T.A. Nijhuis, A.E.W. Beers, F. Kapteijn, J.A. Moulijn, Chem. Eng. Sci. 57 (2002) 1627–1632.
[17] Y.C. Yang, S.R. Vali, Y.H. Ju, J. Chin. Inst. Chem. Eng. 34 (2003) 617–623.
[18] W.M. Van Rhijn, D.E. De Vos, B.F. Sels, W.D. Bossaert, P.A. Jacobs, Chem. Commun. (1998) 317–318.
[19] I. Dıaz, C. Marquez-Alvarez, F. Mohino, K. Prez-Pariente, E. Sastre, J. Catal. 193 (2000) 283–295.
[20] Y. Zheng, X. Su, X. Zhang, W. Wei, Y. Sun, Stud. Surf. Sci. Catal. 156 (2005) 205–212.
[21] B. Rac, A. Molnar, P. Forgo, M. Mohai, I. Bertoti, J. Mol. Catal. A. Chem. 244 (2006) 46–57.
[22] K.A. Connors, Chemical Kinetics: The Study of Reaction Rate in Solution, VCH Publisher Inc, New York, 1990.
[23] J.M. Smith, Chemical Engineering Kinetics, 3rd edition, Mc-Graw Hill, Singapore, 1981.

[24] W.D. Bossaert, D.E.D. Vos, W.M.V. Rhijn, J. Bullen, J. Catal. 182 (1999) 156–164.
[25] J.P. Blitz, C.P. Little, Fundamentals and Applied Aspects of Chemically Modified Surfaces, Royal Society of Chemistry, United Kingdom, 1999.
[26] J. Dhainaut, J.P. Dacquin, A.F. Lee, K. Wilson, Green Chem. 12 (2010) 296–303.
[27] M.P. Kapoor, S. Inagaki, Bull. Chem. Soc. Jpn. 79 (2006) 1463–1475.
[28] M.P. Kapoor, W. Fujii, Y. Kasama, M. Yanagi, H. Nanbu, L.R. Juneja, J. Mater. Chem. 18 (2008) 4683–4691.
[29] S. Inagaki, S. Guan, T. Ohsuna, O. Terasaki, Nature 416 (2002) 304–307.
[30] R.I. Kureshy, I. Ahmad, K. Pathak, N.H. Khan, S.H.R. Abdi, R.V. Jasra, Catal. Commun. 10 (2009) 572–575.